

Programmable DNA Self-Assemblies for Nanoscale Organization of Ligands and Proteins

Sung Ha Park,[†] Peng Yin,[†] Yan Liu,[‡] John H. Reif,[†] Thomas H. LaBean,^{*,†} and Hao Yan^{*,‡}

Department of Computer Science, Duke University, Durham, North Carolina 27708, and Department of Chemistry and Biochemistry, Arizona State University, Tempe, Arizona 85287

Received January 27, 2005; Revised Manuscript Received February 25, 2005

ABSTRACT

We demonstrate the precise control of periodic spacing between individual protein molecules by programming the self-assembly of DNA tile templates. In particular, we report the application of two self-assembled periodic DNA structures, two-dimensional nanogrids, and one-dimensional nanotracks, as template for programmable self-assembly of streptavidin protein arrays with controlled density.

The programmed self-assembly of rationally designed molecular structures into patterned superstructures is a major challenge in nanotechnology. In recent years, predictable self-assembly of DNA “smart tiles” to construct periodically patterned lattices has been demonstrated.^{1–7} Structure formation using DNA smart tiles begins with the chemical synthesis of single-stranded DNA oligonucleotides, which when properly annealed, self-assemble into DNA branched-junction building blocks through Watson–Crick base pairing. DNA tiles can carry sticky ends that preferentially match the sticky ends of other particular DNA tiles, thereby facilitating further assembly into tiling lattices. Recent successes in constructing self-assembled two-dimensional (2D) DNA tiling lattices composed of tens of thousands of tiles may lead to potential applications including nanoelectronics, biosensors, and programmable/autonomous molecular machines. The diversity of materials with known DNA attachment chemistries considerably enhances the attractiveness of DNA tiling assembly, which can be used to form superstructures upon which other materials may be assembled.^{8–15}

We have recently demonstrated the construction of a family of DNA tiles known as four-by-four (4×4) tiles⁷ which resemble a cross structure composed of four 4-arm DNA branch junctions. Self-assembly from a single unit of the cross structure resulted in 2D nanogrids that display periodic square cavities. Periodic protein arrays were also achieved by templated self-assembly of streptavidin (STV)

onto each DNA tile containing biotinylated oligonucleotides.⁷ This work was a proof of the essential capability of using self-assembled DNA nanostructures to scaffold other molecular components. However, there remains the further challenge of programming the self-assembly of the DNA templated protein array with controlled spatial distance and increasing pattern complexity. Fully programmable DNA templated protein arrays, where individual proteins can be positioned with precision and specificity, could allow us to build functional protein templates with nanometer dimensions for single molecule detection. Such assemblies may also prove useful for future nanoscale “factories” by positioning enzymes at desired locations according to their functions to allow sequential reactions on substrates in a flow. Precisely controlled organization of protein molecules onto periodic 2D DNA lattices could also enable us to gain insights into protein structure using 2D cryoelectron microscopy diffraction.

Here we demonstrate the precise control of periodic spacing between individual protein molecules by programming the self-assembly of DNA tile templates. In particular, we report the application of two self-assembled periodic DNA structures, 2D nanogrids and one-dimensional (1D) nanotracks, as template for programmable self-assembly of streptavidin protein arrays (see Supporting Information Figures S1 and S2 for details of the nucleotide sequences). These programmable protein assemblies utilize a two-tile system (A tile and B tile) as selectable templates for protein binding where A tile and B tile associate with each other alternatively through rationally designed sticky ends and self-assemble into either 2D nanogrids or 1D nanotracks (see

* Corresponding authors. E-mail: hao.yan@asu.edu; thl@cs.duke.edu.

[†] Duke University.

[‡] Arizona State University.

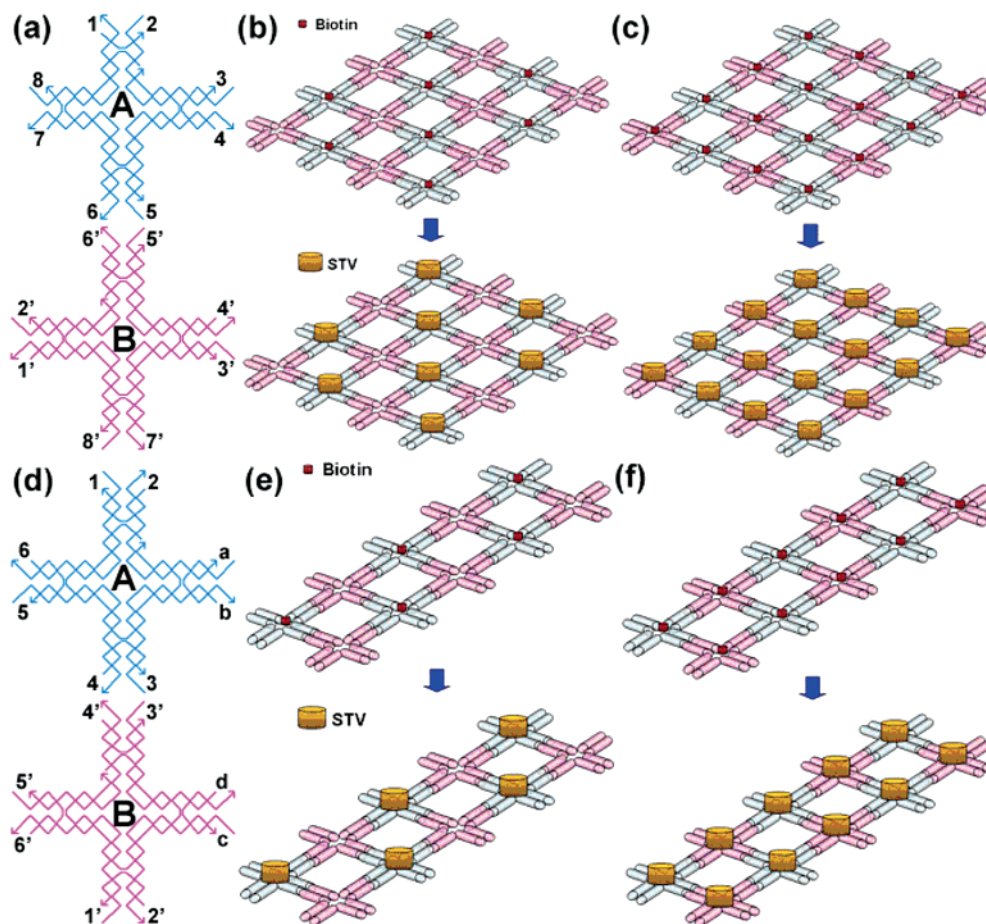


Figure 1. Schematic drawings of the precisely controlled protein self-assembly on programmable DNA scaffolds. (a) Strand structure of 4×4 tiles A (blue) and B (pink) for the construction of the 2D nanogrids. Complementary sticky end pairs are labeled as n and n' . (b and c) Schematic cartoons of the AB tile self-assembly and subsequent binding of streptavidin onto A^*B lattice and A^*B^* lattice, respectively. Biotin groups and streptavidin molecules are represented as smaller red dots and larger yellow cylinders, respectively. (d) Strand structure of 4×4 tiles A (blue) and B (pink) for the construction of the 1D AB nanotrack. Complementary sticky end pairs are labeled as n and n' . In contrast, a , b , c , and d are noncomplementary sticky ends. (e and f) Illustrate schematic cartoons for the self-assembly of streptavidin templated by 1D A^*B nanotrack and A^*B^* nanotrack, respectively.

Supporting Information Figures S3 and S4 for details of the sticky end arrangements and tile corrugation scheme). A tile and B tile can be selectively modified such that either one or both tile types carry biotin groups. In consequence, the combination of selectively modified A and B tiles in the self-assembly and subsequent binding of streptavidin to biotin leads to varied periodic spacing of the protein molecules on the DNA lattices.

Figure 1a, b, and c illustrate schematic drawings of the AB tile system for the 2D nanogrid assembly and the subsequent streptavidin attachment to form two distinct protein arrays. The basic DNA building blocks, A tile and B tile (Figure 1a), were derived from the aforementioned 4×4 tile.⁷ Each A and B tile contains four 4-arm DNA branched junctions pointing in four directions (north, south, east, and west in the tile plane). Each tile is composed of nine strands, with a central strand participating in all four junctions. The sticky ends of A and B tiles are designed such that complementary sticky end pairs are indicated as numbers n and n' . The association of the programmed sticky ends between A and B tiles will result in a 2D lattice composed of alternating A and B tiles, as shown in Figure 1b and c.

To template the assembly of streptavidin molecules, the loops at the center of the A and B tiles were selectively modified to incorporate a biotin group indicated as a red dot in just A tile as shown in Figure 1b or in both A and B tiles as shown in Figure 1c. Biotinylated A and B tiles are denoted as A^* and B^* , respectively. The lattice in Figure 1b is composed of A^* tile and B tile and hence is denoted as A^*B lattice, while the one in Figure 1c consisting of A^* and B^* tiles is denoted as A^*B^* lattice. The binding of streptavidin (indicated as yellow cylinders) to the biotin sites in A^*B lattice or A^*B^* lattice results in two distinct forms of streptavidin nanoscale arrays with different periodic spacing between adjacent protein molecules. Streptavidin on A^*B^* nanoarray is designed to be twice as dense as A^*B arrays.

A system of programmable protein arrays with increasing complexity would benefit from an ability to design various DNA templates from an identical core structure. By keeping the core structure of the 4×4 AB tiles and intentionally introducing noncomplementarity into the sticky ends on one side of the A and B tiles (indicated as sticky ends a , b , c , and d in Figure 1d), self-assembly of 1D DNA nanotrack (Figure 1e and f) can be obtained. Again, selective biotin

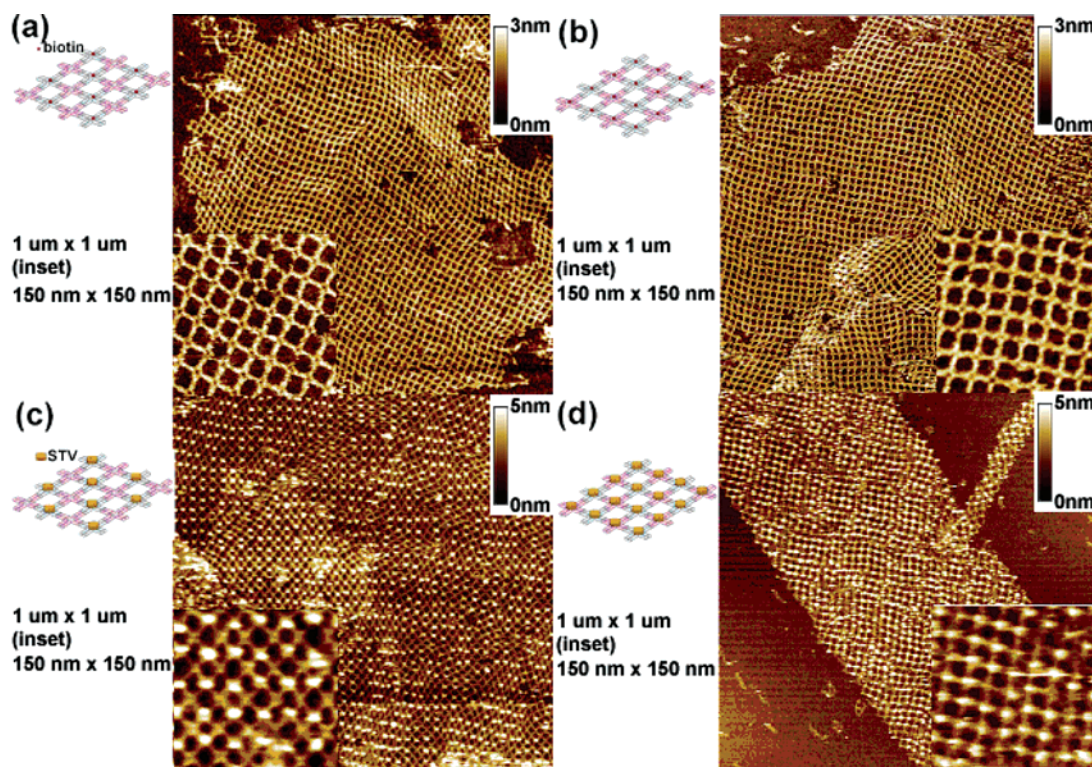


Figure 2. Atomic force microscopy images of the programmed self-assembly of streptavidin on 2D DNA nanogrids. (a and b) AFM images of bare A*B and A*B* nanogrids before streptavidin attachment. (c and d) AFM images obtained after binding of streptavidin to the bare DNA nanogrids A*B and A*B*, respectively. Scan sizes of all AFM images are $1\ \mu\text{m} \times 1\ \mu\text{m}$ with $150\ \text{nm} \times 150\ \text{nm}$ zoom-in insets.

incorporation into the central loop of the AB tile system results in two forms of nanotracks: A*B nanotracks (Figure 1e), where only tile A is biotinylated; A*B* nanotracks (Figure 1f), where both tile types are biotinylated. Streptavidin binding to these two forms of nanotracks in turn results in two distinct self-assembled streptavidin arrays, as shown in Figure 1e and f.

Following formation of lattice and subsequent binding of streptavidin, the lattices were examined by atomic force microscopy (AFM) imaging. Figure 2a and b are AFM images of the bare 2D A*B DNA nanogrids and A*B* DNA nanogrids, respectively. Figure 2c and 2d show the two distinct forms of protein nanoarrays resulting from streptavidin binding to lattices A*B and A*B*, respectively. Streptavidin has a diameter of $\sim 4\ \text{nm}$. Its binding to the self-assembled A*B and A*B* arrays generates topographical features on the mica surface that are higher than bare DNA lattices and are visualized as brighter bumps at the appropriate tile centers. AFM images in both Figure 2c and 2d clearly demonstrate the regular periodicity of the streptavidin molecules templated on the 2D DNA nanogrids. The measured average distance between pairs of adjacent streptavidin molecules is about $\sim 36.9\ \text{nm}$ in Figure 2c and $\sim 18.5\ \text{nm}$ in Figure 2d, which is in good agreement with the designed parameters. AFM height measurements show that STV molecules in Figure 2c and 2d have an average height of $\sim 3.8\ \text{nm}$, compared to the height of $\sim 1.4\ \text{nm}$ measured on bare DNA lattices in Figures 2a and 2b. This further confirms that the periodic bumps in the lattice result from the binding of streptavidin to the DNA tiles. In our

design, the biotin labels are located on the T₄ flexible linkers within the small cavity at the center of the 4×4 tiles and are not designed to be specifically on one face of the tile. Therefore, strictly alternating placement of bound streptavidin either above or below the lattice plane is not necessarily expected. Furthermore, the DNA lattice is sufficiently flexible that AFM imaging of the topographic features of the lattice might not be able to differentiate between proteins bound above versus below the DNA. As it is well-known that streptavidin has four binding sites for biotin, therefore the binding of streptavidin to DNA lattice could lead to cross-link between multiple layers of the DNA lattice. To avoid such possible scenario, the stoichiometry was controlled specifically to avoid cross-linking. Streptavidin was added at a molar ratio of 1:1 compared to DNA-bound biotin, therefore the binding of multiple biotin moieties by any single STV tetramer was minimized.

The formation of a 1D AB nanotracks and the subsequent binding of streptavidin were also confirmed with AFM imaging. Figures 3a and 3b are AFM images of the bare 1D A*B DNA nanotracks and A*B* DNA nanotracks, respectively. Figures 3c and 3d show the two distinct forms of protein arrays resulting from streptavidin binding to nanotracks A*B and A*B*, respectively. The measured average distance between each pair of adjacent streptavidin molecules is about $\sim 36\ \text{nm}$ in Figure 3c and $\sim 18\ \text{nm}$ in Figure 3d, which is in good agreement with the designs. AFM height measurements again reveal the binding of streptavidin compared to bare DNA nanotracks in Figures 3a and 3b and provide clear evidence that the assemblies formed as

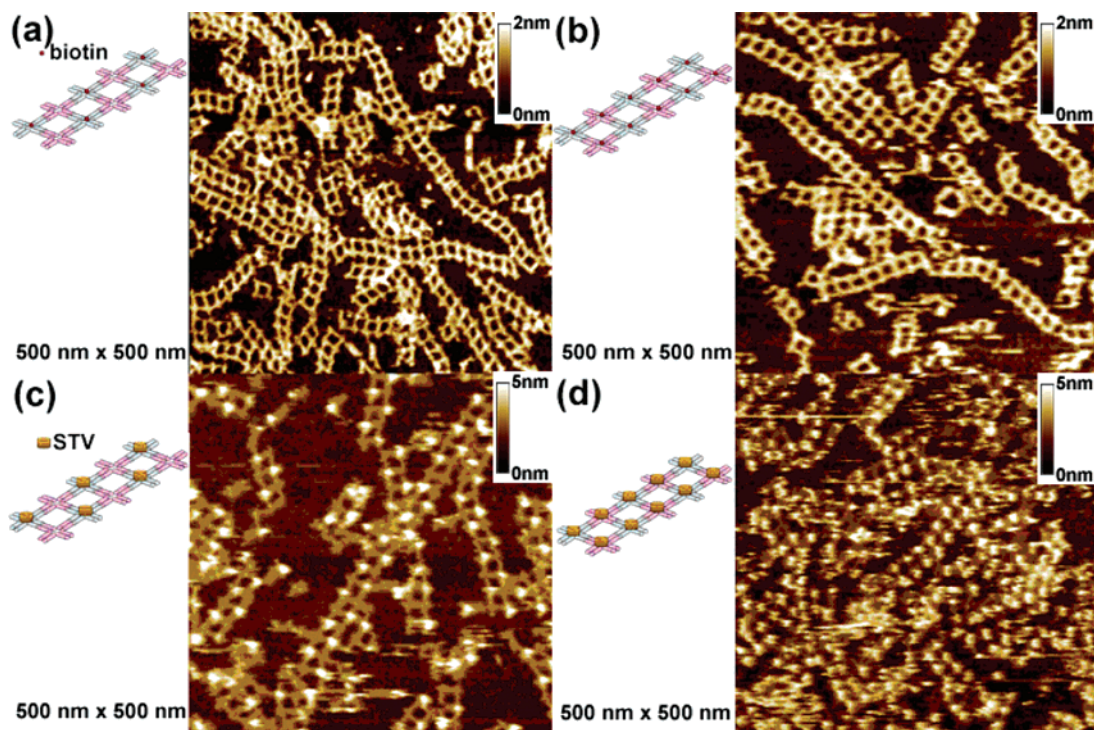


Figure 3. Atomic force microscopy images of the programmed self-assembly of streptavidin on 1D DNA nanotracks. (a and b) AFM image of bare A*B and A*B* nanotracks before streptavidin binding, respectively. (c and d) AFM image of A*B and A*B* nanotracks after binding of streptavidin. All AFM images are 500 nm \times 500 nm.

designed. Both nanotracks and nanogrid structures formed with very high reproducibility (as demonstrated further in Supporting Information Figure S5).

In summary, we have rationally designed, assembled, and examined a set of programmed self-assembling nanostructures. We have made 2D and 1D protein arrays with precisely controlled spacing and periodicity templated on two types of DNA nanoassemblies, the 2D nanogrid and 1D nanotracks. This is one step forward toward more programmable and complex assembly of protein arrays at the nanoscale. Fine-tunable and programmable protein arrays of this kind can provide a useful platform for other scientific investigations, for instance, in the study of macromolecular interactions with controlled distance between interacting proteins, as well as a powerful approach for nanofabrication, in particular for complex molecular architectures. Recent work by Chworos et al.¹⁶ and Rothmund et al.¹⁷ demonstrated the use of nucleic acid nanostructures to construct more complex superstructures. This makes the construction of complex protein nanoassemblies a more realistic objective.

Experimental Section. DNA sequences were designed and optimized with the SEQUIN¹⁸ software and are listed in the Supporting Information. DNA and biotinylated DNA oligos were synthesized by Integrated DNA Technology, Inc. (www.idtdna.com) and purified by denaturing polyacrylamide (15%) gel electrophoresis. The concentrations of DNA oligos were determined by the ultraviolet absorption at 260 nm wavelength. For DNA tiling assemblies, individual DNA oligos were mixed together stoichiometrically at 1.0 μ M in 1 \times TAE/Mg²⁺ buffer (40 mM Tris-HCl (pH 8.0), 20 mM acetic acid, 2 mM EDTA, and 12.5 mM magnesium acetate)

and slowly cooled from 95 to 20 $^{\circ}$ C over a period of 2 days. Streptavidin was purchased from Rockland, Inc. (www.rockland-inc.com). 30 μ L of the preannealed 1.0 μ M DNA structure was mixed with 30 μ L of the 1.0 μ M solution of streptavidin for an hour at room temperature, then incubated overnight at 4 $^{\circ}$ C before imaging. For AFM imaging, 5 μ L sample was spotted on freshly cleaved mica for 5 min. 30 μ L 1 \times TAE/Mg²⁺ buffer was then placed onto the mica and another 30 μ L of 1 \times TAE/Mg²⁺ buffer was placed onto the AFM tip. AFM images were obtained on a Digital Instruments Nanoscope IIIa with a multimode head by tapping mode under buffer using NP-S tips (Veeco Inc.).

Acknowledgment. This work has been supported by grants from NSF (CCF-0453686, CCF-0453685) and faculty start-up fund from ASU to Hao Yan, and NSF (EIA-0218376, CCR-0326157) to Thomas H. LaBean. We thank Jie Liu for the use of the Nanoscope IIIa.

Supporting Information Available: DNA sequences, experimental methods, additional AFM images and image analysis. This material is available free of charge via the Internet at <http://pubs.acs.org>.

References

- (1) Seeman, N. C. *Nature* **2003**, *421*, 427.
- (2) Winfree, E.; Liu, F.; Wenzler, L. A.; Seeman, N. C. *Nature* **1998**, *394*, 539.
- (3) Mao, C.; Sun, W.; Seeman, N. C. *J. Am. Chem. Soc.* **1999**, *121*, 5437.
- (4) LaBean, T. H.; Yan, H.; Kopatsch, J.; Liu, F.; Winfree, E.; Reif, J. H.; Seeman, N. C. *J. Am. Chem. Soc.* **2000**, *122*, 1848.
- (5) Sha, R.; Liu, F.; Millar, D. P.; Seeman, N. C. *Chem. Biol.* **2000**, *7*, 743.

- (6) Yan, H.; LaBean, T. H.; Feng, L.; Reif, J. H. *Proc. Natl. Acad. Sci. U.S.A.* **2003**, *100*, 8103.
- (7) Yan, H.; Park, S. H.; Finkelstein, G.; Reif, J. H.; LaBean, T. H. *Science* **2003**, *301*, 1882.
- (8) Alivisatos, P. A. *Nature* **1996**, *382*, 609.
- (9) Jin, R.; Wu, G.; Li, Z.; Mirkin, C. A.; Schatz, G. C. *J. Am. Chem. Soc.* **2003**, *125*, 1643.
- (10) Niemeyer, C. M.; Koehler, J.; Wuerdemann, C. *ChemBioChem* **2002**, *3*, 242.
- (11) Loweth, C. J.; Caldwell, W. B.; Peng, X.; Alivisatos, A. P.; Schultz, P. G. *Angew. Chem. Int. Ed.* **1999**, *38*, 1808.
- (12) Zanchet, D.; Micheel, C. M.; Parak, W. J.; Gerion, D.; Alivisatos, A. P. *Nano Lett.* **2001**, *1*, 32.
- (13) Xiao, S.; Liu, F.; Rosen, A.; Hainfeld, J. F.; Seeman, N. C.; Musier-Forsyth, K. M.; Kiehl, R. A. *J. Nanopart. Res.* **2002**, *4*, 313.
- (14) Le, J. D.; Pinto, Y.; Seeman, N. C.; Musier-Forsynth, K.; Taton, T. A.; Kiehl, R. A. *Nano. Lett.* **2004**, *4*, 2343.
- (15) Li, H.; Park, S. H.; Reif, J. H.; LaBean, T. H.; Yan, H. *J. Am. Chem. Soc.* **2004**, *126*, 418–419.
- (16) Chworos, A.; Severcan, I.; Koyfman, A. Y.; Weinkam, P.; Oroudjev, E.; Hansma, H. G.; Jaeger, L. *Science* **2004**, *306*, 2068.
- (17) Rothmund, P. W. K.; Papadakis, N. P.; Winfree, E. *PLos Biol.* **2004**, *2*, e424.
- (18) Seeman, N. C. *J. Biomol. Struct. Dyn.* **1990**, *8*, 573.

NL050175C